

# The use of video surveys, a Geographic Information System and sonar backscatter data to study faunal community dynamics at Juan de Fuca Ridge hydrothermal vents

Sébastien DURAND<sup>1,2</sup>, Marlène LE BEL<sup>1</sup>, S. Kim JUNIPER<sup>1</sup>  
and Pierre LEGENDRE<sup>2</sup>

<sup>1</sup> GEOTOP – Université du Québec à Montréal, C.P. 8888 succ.  
Centre-Ville-Montréal (Québec), H3C-3P8, Canada

<sup>2</sup> Département des Sciences Biologiques - Université de Montréal, C.P. 6128 succ.  
Centre-Ville-Montréal (Québec), H3C-3J7, Canada

E-mail: [sebastien.durand@umontreal.ca](mailto:sebastien.durand@umontreal.ca)

## Introduction

The study of benthic faunal dynamics in the deep sea is often hampered by technical limitations that include our inability to accurately reconstruct or view areas of seafloor larger than what can be seen through submersible view ports or camera lenses. Manual mapping and image mosaicking have been used with some success to analyse organism distribution within vent sites and at the scale of hydrothermal fields (Juniper *et al.* 1998). In both cases, video or photo transects serve as the primary source of information. Image mosaicking, in principle, is less subjective than mapping by hand, but the present state of the art requires precise control of camera distance and viewing angle to avoid spatial distortion as images are adjusted and fitted into the mosaic (Grehan & Juniper 1996). The reality of operating submersibles over the rugged volcanic and sulphide edifice terrains where hydrothermal vents are found does not always permit collection of imagery suitable for mosaicking, and so manual mapping from video records is still used in some applications (Sarrazin *et al.* 1997). Both techniques yield useful maps that can be used to elucidate relationships between vent organism distribution and habitat features. Time-series mapping with either method can be used to study organism growth, faunal succession, and the response of species and communities to environmental change. Cartographic studies of vent fauna can be further developed by integration of map data into a Geographic Information System (GIS), where a range of powerful, automated spatial analysis tools can be used to explore ecological questions.

This paper reports on a combined hand mapping and GIS approach that we have been using to study

early faunal community dynamics at Cloud Vent, a new hydrothermal site created by a January 1998 eruption on Axial Volcano, on the Juan de Fuca Ridge. We also report on preliminary results of organism and substratum differentiation in sonar backscatter signals, and consider their complementarity with visual imagery. Sonar backscatter analysis offers a potential for automated, swath mapping of habitat over large areas of seafloor, at scales that go well beyond what can be practicably achieved with visual imagery. Seafloor geological and biological features influence the strength and temporal distribution of the acoustic signal that is reflected back to the detector (the first echo), according to their respective densities and textures.

## Material and Methods

### *Study sites*

Cloud Vent (45°56'00"N-129°58'53"W) is located on the South-East of Axial Volcano caldera (46° N-130° W) on the Juan de Fuca Ridge, 200 nautical miles off the British-Columbia coast. The site is 1500 m deep and covers a 12m x 10m area of shallow collapse in the central portion of the lava flow generated by the January 1998 eruption. This site was the focus of our video transects and GIS mapping study.

Sonar backscatter experiments were conducted at Clam Bed (47°57'47"N-129°05'30"W), a larger vent field located on the Endeavour Segment of the Juan de Fuca Ridge. The *circa* 50m x 20m site consists of two roughly parallel 2-3m high north-south trending ridges colonised by tubeworm (*Ridgea piscesae*) and alvinellid polychaete/limpet assemblages. The depression between the ridges is slightly sedimented and hosts vesicomylid clams.

## VIDEO AND SONAR STUDIES ON JFR

### *Image and sonar acquisition*

The Remotely Operated Vehicle ROPOS (ROV) was used for acquisition of all video and sonar imagery. Imagery from the submersible's SIT (Silicon Intensified Targeting) and 3-CCD (Charge-Coupled Device) cameras was recorded to S-VHS or digital (Mini-DV) tapes. Video imagery was recorded during overlapping zigzag imaging transects at Cloud Vent, where the submersible held a constant heading. The SIT video imagery served to determine the general site profile and to reconstruct geological features. The 3-CCD colour camera was used for faunal community identification and characterisation.

### *Mapping and GIS construction.*

Vent faunal distribution maps for 1998, 1999, 2000 and 2001 were constructed following the mapping methods described in Delaney *et al.* (1992), Sarrazin *et al.* (1997) and Sarrazin & Juniper (1998). Briefly, while repeatedly viewing the recorded video transects, visually distinct faunal assemblages were hand drawn on a background geological map that included two reference markers (N4 & N6). Information on the relative density of the faunal assemblages was also incorporated into the distribution maps. Hand drawn maps were then scanned, and imported into a graphics program (Freehand®) where the distribution of each faunal assemblage was traced into a separate layer, along with relative density information. Each layer was then imported into the GIS as separate a georeferenced layer, then integrated into a single GIS using Idrisi® software. Each layer was georeferenced using the positions of the visible markers, and transect beginning and end positions, as determined by the submersible's long baseline navigation system (using the Universal Transverse Mercator, Zone 9 North "UTM-9N" coordinate system). As a result of the resampling or "georeferencing" process, the initial image files were stretched and rotated in order to fit the mapping projection (UTM-9N), thus generating directly comparable maps.

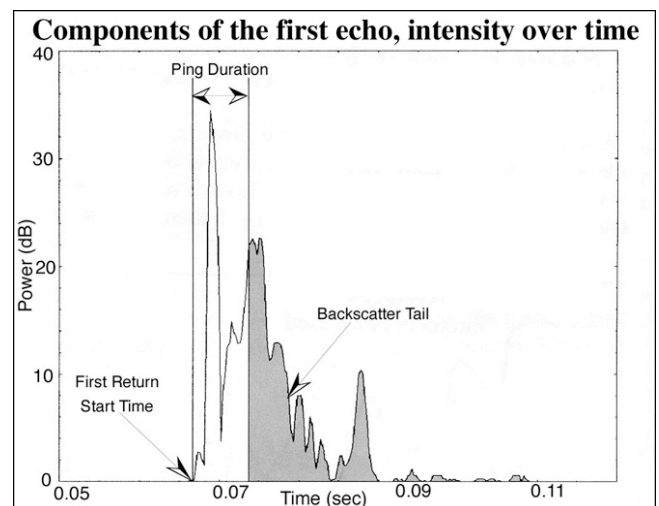
### *Sonar Backscatter Experiments*

Sonar backscatter investigations used an Imagenex 881 mechanical scanning sonar, which has a resolution of 0.15°, a pencil beam of 1.7°, a frequency of 675 kHz and a maximum range of 100 m. In order to evaluate the ability of the sonar to distinguish between different bottom types and different benthic communities, we conducted a series of ground truthing experiments. The submersible was positioned over 5 visually distinct habitat or bottom types in the

Clam Bed field, and sonar data were collected as the vehicle slowly rose vertically from 0m to 25m altitude while insonifying the seafloor below. For these experiments, the sonar head was fixed stationary and facing straight down (zero degree angle). The selected habitat/bottom types were:

- 1) Ridge top without tubeworms
- 2) Ridge top with semi-continuous tubeworm bushes
- 3) Ridge top with dense, continuous tubeworm bushes
- 4) Ridge top with polychaete/limpet assemblages
- 5) Sedimented depression with clams

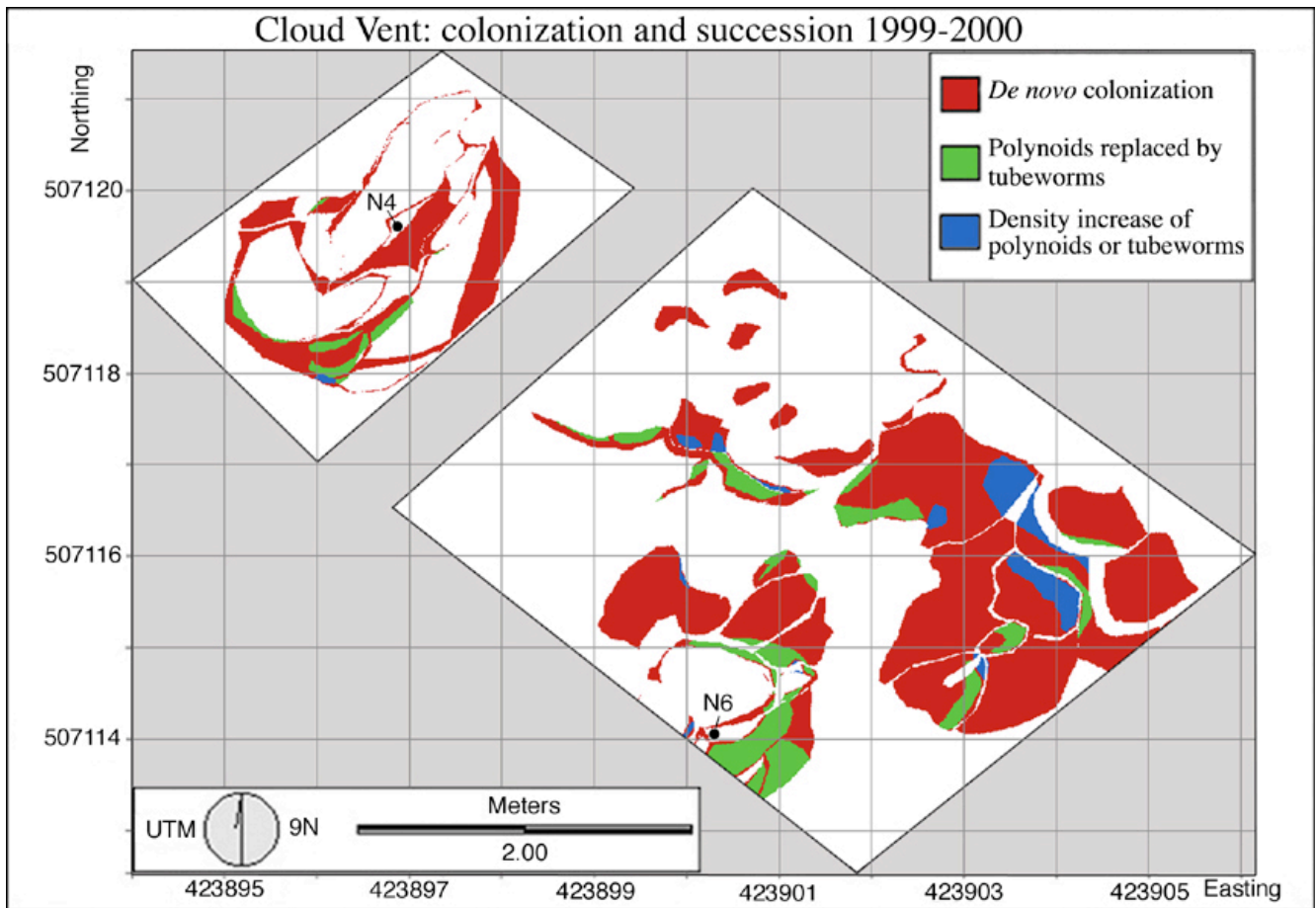
At least 40 acoustic returns for each habitat type, obtained between 2.5 and 3.5m altitude, were included in this preliminary analysis. At this height, the footprint (insonified area) is a 9 cm diameter circle. Once the sonar data were post-processed (filtered for ambient noise, then normalized for depth following Clark & Hamilton 2001), the backscatter tail was extracted from the first echo (Fig. 1) and intensity/time values were analysed using Principal Components Analysis (PCA). The principal components that accounted for 95% of the variation of the original multivariate data were retained for partitioning. K-means partitioning (Legendre *et al.*, 2002) was then performed on the principal components (coordinates of the objects in PCA ordination space) to group the different signature types. The best partition or grouping produced was selected using the Calinski-Harabasz (C-H) criterion, which is a *F*-statistic.



**Figure 1.** Acoustic return (signal strength versus time) detected by the Imagenex 881 sonar head following initiation of a single ping. The backscatter tail (shaded area) is the entire first echo minus the duration of the sonar interrogation ping. The shape of the signal (power fluctuation over time) is a function of bottom texture and density.

**Table 1:** Yearly distribution of polynoid polychaete and tubeworm assemblages within the two mapped zones (N4 and N6) at Cloud Vent, Axial Volcano. Data are percentages of the area in each zone occupied by the two assemblages.

YEAR	N4 (11.56 m <sup>2</sup> )			N6 (34.76 m <sup>2</sup> )			TOTAL AREA (46.32 m <sup>2</sup> )		
	1999	2000	2001	1999	2000	2001	1999	2000	2001
Polynoids (%)	29.33	37.55	13.02	10.14	6.75	1.81	14.93	14.44	4.61
Tubeworms (%)	0.66	7.05	5.05	3.60	27.31	14.55	2.87	22.25	12.18
Total area covered (%)	29.99	44.59	18.06	13.74	34.07	16.36	17.80	36.69	16.79

**Figure 2:** Map of Cloud Vent showing the zones where polynoids and tubeworms increased in density, as well as the successional changes between these two faunal assemblages during the 1999-2000 period. 1.6% of this area showed simple density increases of these two communities over the 1-year interval, while on 3.6% of the surface polynoids were replaced by tubeworms, and 24.0% of the study area was colonised *de novo* by tubeworms.

## Results and Discussion

Poor visibility in some years limited visual mapping to separate zones around the two markers placed in 1998. The zones were estimated to be 11.6m<sup>2</sup> (marker N4) and 36.8m<sup>2</sup> (marker N6) in area. Two visually distinct faunal assemblages were identified and mapped during the 4 years of the study. Although the composition of the assemblages has not been formally described, we designated them as the polynoid polychaete and tubeworm assemblages. The polynoid

assemblage, which was the first to appear (1999), was dominated by the polynoid polychaete *Branchinotogluma sp.*. The tubeworm assemblage, which did not appear until the 2000 was dominated by the vestimentiferan *Ridgea piscesae*, the alvinellid polychaete *Paralvinella pandorae*, *Branchinotogluma sp.* and the limpet *Lepetodrilus fucensis* (J. Marcus, University of Victoria, personal communication).

Once the faunal distribution information was incorporated into the GIS, different analytical software tools were used to study the spatial and

## VIDEO AND SONAR STUDIES ON JFR

temporal relationships between the species, and between species and their environment. Table 1 summarizes the year-to-year distribution of the polynoid and tubeworm assemblages in the mapped zones around markers N4 and N6.

### *Overall trend*

In the summer of 1998, approximately 8 months after the eruption that created Cloud Vent, there were no visible faunal assemblages in the zones around the two markers. The following year, the visible macrofauna in both zones consisted almost entirely of polynoid polychaetes, with a few rare patches of tubeworms (Table 1). By 2000, the faunal compositions of zones N4 and N6 had begun to diverge. At N4, more substratum was still occupied by polynoid assemblages than by tubeworms, while at N6 tubeworms became the dominant group. In the final year of the study, there was no noticeable shift in dominant groups in either zone but there was a general decrease in areal occupation by all faunal assemblages. This observation is compatible with an observed overall decrease in hydrothermal outflow at this site (S. Durand & M. Le Bel, personal observation).

### *Density increases and succession (1999-2000)*

We undertook a detailed analysis of the progression of faunal colonization in the 1999-2000 interval, during which the most significant biological changes occurred at the site. In this analysis, we asked three questions of the database: 1) Did further *de novo* colonization of previously bare surfaces occur during this interval? 2) To what extent was the initial polynoid polychaete assemblage replaced by vestimentiferan tubeworms? 3) Were there areas where the initial (mostly polynoid) assemblage remained dominant and increased in density?

The results of these analyses are summarised in Figure 2. The dominant change during the 1999-2000 interval was *de novo* colonization of bare surfaces by tubeworm assemblages. We found that 24.0% of the study area was colonised *de novo* by tubeworms between 1999 and 2000, while only 3.6% of the surface occupied by polynoid assemblages was taken over by tubeworms. A further 1.6% of the total analysed area simply showed density increases for the assemblage present in 1999.

### *Density decrease and senescence (2000-2001)*

We undertook a second interrogation of the database in order to evaluate the consequences of a noticeable

decrease of hydrothermal activity in the 2000-2001 interval. Our initial questions were similar to the above consideration of density increases and succession: 1) To what extent did existing communities simply decrease in density? (2.4% of the colonised surface), 2) To what extent were tubeworms replaced by polynoids (8.4% of colonised surface) 3) To what extent did the fauna disappear altogether (20.8% of the total faunal colonised surface)?

The greatest change in the 2000-2001 interval involved the complete disappearance of existing faunal assemblages (not shown). Slightly more than 20% of the previously colonised surface was bare in 2001. On a further 8.4% of the colonised surface, tubeworm assemblages were replaced by polynoids. With respect to the latter point, we note that the dominant species in the polynoid assemblage (*Branchinotogluma sp.*) was also present and abundant in the tubeworm assemblage. Thus the "replacement" likely involved, to a large extent, the disappearance of the tubeworm overstory, as well as the species living on their tubes, to expose the polynoids on the substratum. Finally, for another 2.4% of the surface colonized in 2001, there was a decrease in density of the same faunal assemblage mapped in 2000.

### *Backscatter differentiation*

In the K-means analysis, the tubeworm backscatter signatures (dense bushes and semi-continuous bushes, Fig. 3) were distinguished as a separate group in the 2-group K-means solution. At that level (C-H statistic = 197.91) (not shown in the form of a table), most of the backscatter signatures of the dense (97%) and semi-continuous tubeworm bushes (86%) were grouped together. In the 4-group solution (C-H = 147.82) the clams and polychaete/limpet assemblages had about 40% of their signatures in a group that they shared with the broken sheet flow (Table 2). The clam and polychaete/limpet assemblages also had identical percentages (58%) in a second group (Table 2). The lava flow and the dense tubeworm bushes each had a major portion of their backscatter signatures in a single group (respectively 74% and 94%). The semi-continuous tubeworms habitat had a less distinct backscatter signature, with 25%, 61% and 13% of its echos divided among three groups. These preliminary results indicate that sonar backscatter analysis has considerable potential for mapping habitat distribution in larger hydrothermal vent fields or seep environments where there is extensive coverage by tubeworm assemblages.

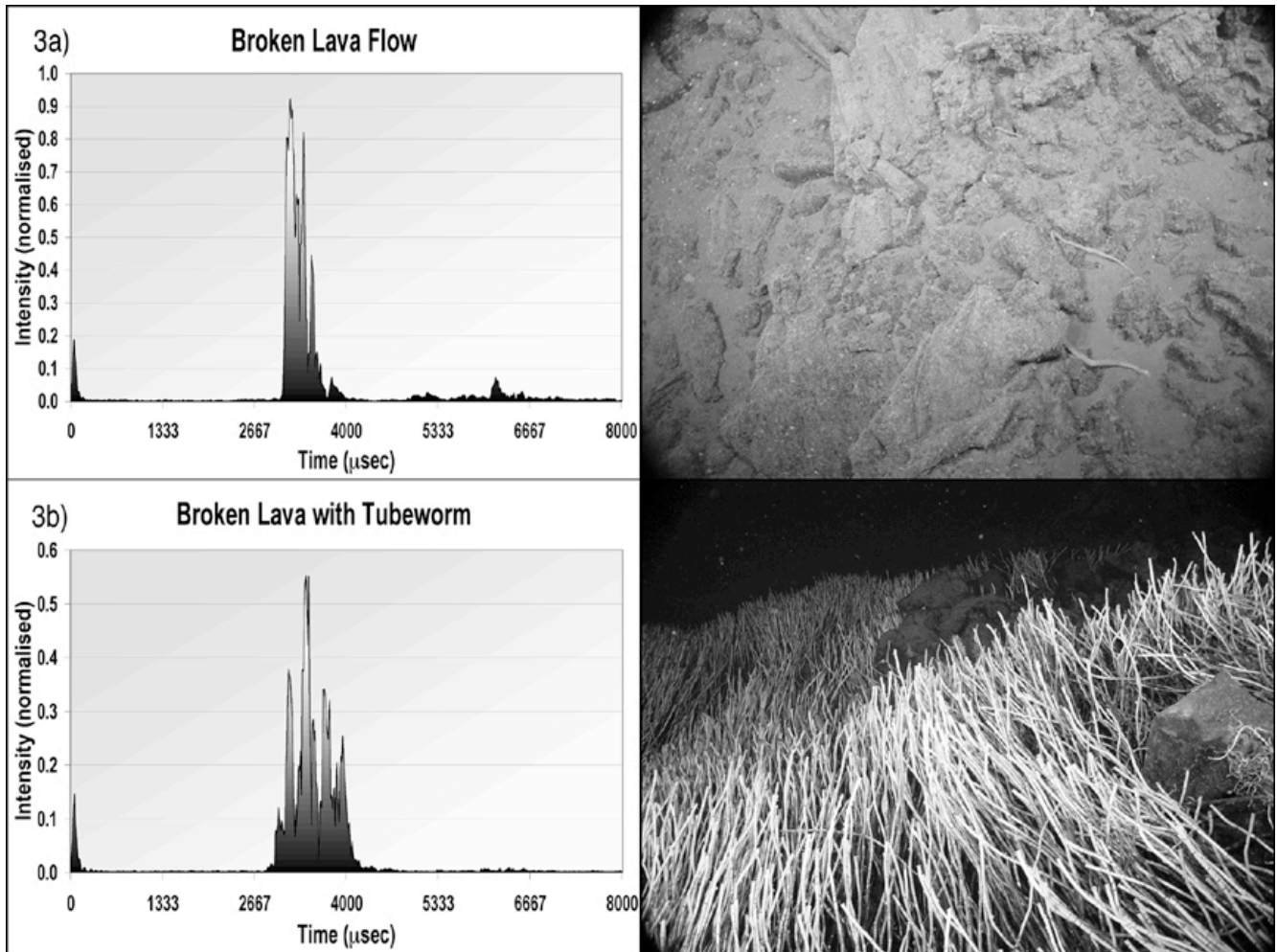


**Figure 3.** Example of contrasting habitat types and backscatter signatures at Clam Bed vent. a) Broken sheet lava flow signature (photograph of site on right). b) Acoustic signature of dense tubeworm bush (photograph on right). These sites were adjacent to each other on a ridge summit. The substratum beneath the tubeworm bush was similar to the broken sheet lava flow shown in (a).

**Table 2.** Results of K-means partitioning of backscatter signatures for the 5 studied habitats. The 2 and 4 group solutions represented local maxima of the Calinski-Harabasz criterion. The 4-group solution described in this table provided the best separation of habitat types. Data for each habitat type (columns of the table) indicate the percentage of the total number of backscatter signatures for that habitat that belong to each of the 4 groups. Values above 50% are in bold.

Grouping	Broken sheet flow	Dense tubeworms	Clams	Limpets	Semi-continuous tubeworms
1	15	03	58	58	13
2	74	0	42	40	01
3	08	03	0	02	61
4	04	94	0	0	25

At this point in our analyses, we do not know whether or not assemblages of smaller-vent organisms will be distinguishable from the surrounding basaltic substratum. Application of this method to more complex terrains will be more difficult. The Clam Bed site was selected for this study because it offered a

relatively flat bottom and contains no mineral edifices. This avoided any confounding effects of relief on the backscatter signal.

The combination of mapping and GIS analysis allowed us to quantitatively compare the importance of the processes of *de novo* colonization and faunal

disappearance at Cloud Vent in relation to shifts in assemblage composition or density. While we cannot exclude the possibility that intermediate stages occurred between our 1-year observation intervals, the data show that the rapid appearance and disappearance of fauna dominated the changes that occurred during the 4 years following the creation of Cloud Vent. In a study of another eruption and colonization event on the Juan de Fuca Ridge, Tunnicliffe *et al.* (1997) observed extensive blooms of bacterial mats followed by colonization by tubeworm assemblages. These authors suggested that microbial mats might be a necessary precursor to colonization of bare rock surfaces by tubeworms. In our 1998 video surveys, bacterial mats could be seen throughout the study area. However, the poor visibility caused by the voluminous venting of fluids rich in suspended particles prevented the systematic mapping of bacterial mat distribution. By 1999, one year before the appearance of extensive tubeworm assemblages at Cloud Vent, the bacterial mats had largely disappeared. This observation would argue against the necessity of any precursor colonization by microbial mats before the arrival of tubeworms. However, the presence or absence of thin bacterial films that might attract tubeworm larvae cannot be confirmed from video observations.

### Conclusion

Video mapping and sonar backscatter analysis are non-interventive techniques well suited to time series studies of the rapidly evolving faunal communities that develop around deep-sea hydrothermal vents. The integration of map data into a GIS, as briefly described here, greatly enhances the power of this information for the exploration of ecological questions. Sonar backscatter information, in addition to not being hampered by lighting and visibility problems, offers the advantage of permitting 3-dimensional reconstruction of habitat distribution on the seafloor using topographical and backscatter information. However, there are still a number of outstanding questions concerning the applicability of sonar backscatter studies to the hydrothermal vent environment, including habitat signature variability and the detection of patchy colonization of hard substrata that so often characterizes vent communities. We are presently investigating these questions at the Cloud Vent and Clam Bed sites.

### Acknowledgements

This work would not have been possible without the field support of the NeMO Chief Scientist. R. Embley, the ROPOS submersible pilots and the crews of the NOAA Ship Ronald H. Brown, the CCGS John P. Tully, and the R/V Thomas G. Thompson. This research was sponsored by NSERC (Canada) Collaborative Research Opportunities grants to SKJ and PL, and by the Canadian Scientific Submersible Facility. ML was supported by an NSERC Canada Undergraduate Research Fellowship. We are particularly grateful to L. J. Hamilton (backscatter analysis), D. Marcotte (Kriging methods), M. Fellows (Imagenex surveys), J. Illman (navigation software training), and J. Marcus (faunal assemblage information).

### References

- Clarke P.A. & Hamilton L.J. 2001.** The ABCS program for the analysis of echo sounder returns for acoustic bottom classification. *Defence Science and Technology Organisation*, DSTO-GD-0215.
- Grehan A. & Juniper S.K. 1996.** Clam distribution and subsurface hydrothermal processes at Chowder Hill (Middle Valley), Juan de Fuca Ridge. *Marine Ecology Progress Series*, **130**: 105-115.
- Juniper S.K. Sarrazin J. & Grehan A. 1998.** Remote sensing of organism density and biomass at hydrothermal vents. *Cahiers de Biologie Marine*, **39**: 245-247.
- Legendre, P., K.E. Ellingsen, E. Bjørnbom & Casgrain P. 2002.** Acoustic seabed classification: improved statistical method. *Canadian Journal of Fisheries and Aquatic Sciences* **59**: 1085-1089.
- Sarrazin J. & Juniper S.K. 1998.** The use of video imagery to gather biological information at deep-sea hydrothermal vents. *Cahiers de Biologie Marine*, **39**: 255-258.
- Sarrazin J., Robigou V., Juniper S.K. & Delaney J.R. 1997.** Biological and geological evolution over four years on a high temperature hydrothermal structure, Juan de Fuca Ridge. *Marine Ecology Progress Series*, **153**: 5-24.
- Tsurumi, M. 2001.** The application of Geographical Information Systems to biological studies at hydrothermal vents. *Cahiers de Biologie Marine*, **39**: 263-266.
- Wright, D.J. 1994.** Geographic Information System for RIDGE research. *Ridge Events*, **5**(2): 5-7.